UNIVERSITÀ DEGLI STUDI DI BERGAMO
DIPARTIMENTO DI INGEGNERIA

QUADERNI DEL DIPARTIMENTO

Department of Engineering

Working Paper

Series "*Mathematics and Statistics*"

n. 01/MS – 2013

PATIENT-SPECIFIC GENERATION OF THE PURKINJE NETWORK DRIVEN BY CLINICAL MEASUREMENTS

by

C. Vergara, S. Palamara, D. Catanzariti, C. Pangrazzi, F. Nobile, M. Centonze, E. Faggiano, M. Maines, A. Quarteroni, G. Vergara

[§] L'accesso alle *Series* è approvato dal Comitato di Redazione. I *Working Papers* della Collana dei Quaderni del Dipartimento di Ingegneria dell'Informazione e Metodi Matematici costituiscono un servizio atto a fornire la tempestiva divulgazione dei risultati dell'attività di ricerca, siano essi in forma provvisoria o definitiva.

PATIENT-SPECIFIC GENERATION OF THE PURKINJE NETWORK DRIVEN BY CLINICAL MEASUREMENTS

Christian Vergara, Dipartimento di Ingegneria, Università di Bergamo, viale Marconi 5, 24044 Dalmine (BG), Italy

Simone Palamara, MOX, Dipartimento di Matematica, Politecnico di Milano, Piazza Leonardo da Vinci 32, 20131, Milano, Italy

Domenico Catanzariti, Divisione di Cardiologia, Ospedale S. Maria del Carmine, Corso Verona, 4, 38068, Rovereto (TN), Italy

Cesarino Pangrazzi, Divisione di Cardiologia, Ospedale S. Maria del Carmine, Corso Verona, 4, 38068, Rovereto (TN), Italy

Fabio Nobile, Dipartimento di Matematica, Politecnico di Milano, Piazza Leonardo da Vinci 32, 20131, Milano, Italy, and MATHICSE-CSQI, École Polytechnique Fédérale de Lausanne, SB SMA-GE, MA B2 444 (Bâtiment MA), Station 8, CH-1015, Lausanne, Switzerland

Maurizio Centonze, U.O. di Radiologia di Borgo-Pergine, Viale Vicenza 9, 38051 Borgo Valsugana (TN), Italy

Elena Faggiano, MOX, Dipartimento di Matematica, and LaBS, Dipartimento di Chimica, Materiali e Ingegneria Chimica, Politecnico di Milano, Piazza Leonardo da Vinci 32, 20131, Milano, Italy

Massimiliano Maines, Divisione di Cardiologia, Ospedale S. Maria del Carmine, Corso Verona, 4, 38068, Rovereto (TN), Italy

Alfio Quarteroni, MOX, Dipartimento di Matematica, Politecnico di Milano, Piazza Leonardo da Vinci 32, 20131, Milano, and MATHICSE-CSQI, École Polytechnique Fédérale de Lausanne, SB SMA-GE, MA B2 444 (Bâtiment MA), Station 8, CH-1015, Lausanne, Switzerland

Giuseppe Vergara, Divisione di Cardiologia, Ospedale S. Maria del Carmine, Corso Verona, 4, 38068, Rovereto (TN), Italy

Corresponding author: Christian Vergara, Viale Marconi 5, 24044, Dalmine (BG), Italy, Fax: +39 035 2052310; Phone number: +39 035 2052314;
e- mail: christian.vergara@unibg.it

Total number of words: 6511

Number of words of the abstract: 192

Number of figures: 6

Number of tables: 2

ABSTRACT

The propagation of the electrical signal in the Purkinje network is the starting point for the activation of the muscular cells leading to the contraction of the heart. In the computational models describing the electrical activity of the ventricle is therefore important to account for the Purkinje fibers. Until now, the inclusion of such fibers has been obtained by using surrogates such as space-dependent conduction properties or by generating a network based only on an *a priori* anatomical knowledge. Aim of this work was to propose a new method for the generation of the Purkinje network by using clinical measures of the activation times on the endocardium allowing to generate *a patient-specific* network. To assess the accuracy of the proposed method we compared its accuracy with that of other strategies proposed so far in the literature for three cases with a normal electrical propagation. The results showed that with the proposed method we were able to reduce the errors by at least 25% with respect to the best of the other strategies. This highlighted the reliability of the proposed method and the importance of including a patient-specific Purkinje network in computational models.

Keywords: Purkinje fibers, computational methods, activation times, Eikonal equation.

NON-STANDARD ABBREVIATIONS AND ACRONYMS

PF Purkinje fibers, CCS Cardiac conduction system, PMJ Purkinje muscular junctions, MRI Magnetic Resonance Imaging, 3D Three-dimensional, AV Atrioventricular, WPW Wolff–Parkinson–White.

INTRODUCTION

The Purkinje fibers (PF) represent the peripheral part of the cardiac conduction system (CCS) and are located just beneath the endocardium. Their main role consists in providing rapid and coordinate activation of the ventricular myocardium [8], an essential feature for the correct pumping of the blood flow into the arteries. PF are electrically connected to the ventricular muscle only at certain insertion sites, called Purkinje muscle junctions (PMJ) [15]. From these sites the depolarization wave enters the heart muscle, allowing the ventricular excitation and contraction [2].

The mathematical and computational models of cardiac electrophysiology allow to compute virtually the electrical activity in the ventricles [11]. The inclusion of CCS and in particular of the PF in such models is therefore essential to simulate the ventricular activation. While the anatomical reconstruction of the heart geometry is possible thanks to the modern imaging techniques (such as MRI and CT), radiological images do not allow to identify and reconstruct the PF.

Until now, the inclusion of the PF in the computational models has been obtained either by means of surrogates such as the definition of space-dependent conduction properties [20], or by means of the automatic generation of the Purkinje network based on a fractal law and on an *a priori* anatomical knowledge [1,9,18].

In this work, we proposed a method for the generation of a *patient-specific* Purkinje network driven by clinical measures of the activation times on the endocardium of the left ventricle in a normal propagation. At the best of the authors' knowledge, this is the first attempt to use clinical data for the explicit construction of the PF by means of computational models.

To assess the accuracy of the proposed method, we considered clinical measures of three subjects characterized by a normal propagation and we compared the results obtained by our method with those of other strategies proposed so far in the literature.

The purpose of this study was twofold: i) To show the applicability and reliability of our method for the generation of patient-specific Purkinje networks in real cases; ii) To prove the essential

role of a patient-specific Purkinje network in computational models to obtain an accurate description of the normal activation in the left ventricle.

METHODS

Patient-specific clinical measurements

Acquisition of imaging data and reconstruction of the endocardium geometry

We considered three subjects characterized by a normal electrical propagation. Firstly, they underwent Magnetic Resonance Imaging (MRI). Using a 1.5 Tesla MRI Unit (Magnetom Avanto, Siemens Medical Systems, Erlangen, Germany) and a 8 channel phased array torso coil, a non-contrast enhanced three-dimensional (3D) whole heart sequence, cardiac and respiratory gated, was performed using the following parameters: voxel resolution of 1.7x1.6x1.3 mm; TR (repetition Time)=269.46; TE (EchoTime)=1.46 ms; flip angle=90°; slice thickness=1.3 mm with 104 slices per single slab; acquisition matrix=256×173.

Then, the segmented images of the left ventricle endocardium have been obtained by processing the MRI study using the EnSite Verismo™ Segmentation Tool (EnSite Verismo 2.0.1), which is based on a threshold method. Later, the segmented images have been used to build the computational domains in view of the numerical simulations and have been imported into the EnSite NavX system to acquire the activation times.

Acquisition of electrical data

The activation times were measured on the endocardium of the left ventricle in the three subjects by means of the Ensite NavX system. This is capable of accurately locating any electrode catheter within the 3D navigation field, allowing the reconstruction of the mapping of the activation times. As mentioned earlier, in this work we considered only the activation times related to subjects with a normal electrical propagation.

The study has been approved by the ethic committee of Azienda Provinciale per i Servizi Sanitari, Trento, Italy. The subjects have been previously informed and gave their consent both for the invasive clinical procedure and for the successive mathematical elaborations.

Patient-specific generation of the Purkinje fibers network

The normal electrical activity of the left ventricle is characterized by a front propagating through the Purkinje network and then within the heart muscle. In particular, in the normal propagation the front starts from the atrioventricular (AV) node and propagates in the proximal part of the PF with a velocity in the range 3-4 m/s [13]. At the mid-antero-septal level, located on the endocardium, the PF start to be connected with the ventricular muscle cells through the PMJ. In this way, the electrical signal enters the ventricle muscle and propagates in the whole myocardium, with a reduced conduction velocity in the range 0.3-0.8 m/s [13].

General overview of the algorithm

The starting point of our method was the use of a fractal law to generate a *tentative* Purkinje network as proposed in [1,9,18]. Then, such a network has been corrected by using the data of the normal activation acquired with the EnSite NavX system, allowing to obtain a patient-specific network. In particular, our method can be summarized in the following steps:

Generation of the patient-specific Purkinje network using data of a normal propagation and computation of the activation times in the left ventricle:

1) Manually design of the bundle of His and of the main bundle branches;
2) Generation of a *tentative* Purkinje network without using the clinical data;
3) Computation of the activation times in the tentative network and in particular at the PMJ;
4) Computation of the activation times on the endocardium of the left ventricle by using as input the activation times at the tentative PMJ computed at step 3;
5) Comparison between the activation times computed at step 4 and the measured data;

6) Generation of the *patient-specific* Purkinje network as a correction of the tentative one, driven by the discrepancies between the computed and the measured data obtained at step 5;
7) Computation of the activation times in the patient-specific network and in particular at the PMJ;
8) Computation of the activation times in the endocardium (or in whole left ventricle) by using as input the activation times at PMJ computed at step 7.

We notice that the algorithm for the patient-specific Purkinje network generation involves only steps from 1 to 6. Here we have added also steps 7 and 8 for the computation of activation times in the endocardium or even in the whole left ventricle, since this was the final goal of the PF generation. We also observe that at steps 3-4 and 7-8 we firstly solved the network solely (steps 3,7), and then we used this solution evaluated at the PMJ as sources for the computation of the muscular activation (steps 4,8). This is an *explicit* solution strategy, since it does not account for the feedback of the muscular activation on the Purkinje network. This choice was justified by the fact that for a normal electrical activity the propagation in the PF are not influenced by the muscular propagation.

Modeling the electrical activity

We illustrate now the mathematical models used to compute the activation times (steps 3,4,7,8 in our algorithm). One of the most widely used models for the description of the electrical activity in the myocardium is the so-called *bidomain equation*, obtained by considering a propagation both in the extra- and in the intra-cellular spaces [12,24,7] . However, if one is interested only in the activation times, then the simpler Eikonal equation could be considered [10,5]. This is a steady model which allows to recover for any point of the computational domain the activation time at which the potential reaches the value $(W_r+W_p)/2$, where W_r is the minimum of the potential and W_p the value reached at the plateau. This simple model has been often used for clinical applications, see for example the recent work [22].
As observed, the patient-specific clinical data were available only on the endocardium. For this reason, in view of the comparison between computed and measured data at step 5 of our algorithm, we needed to know the computed activation times only on the endocardium. Then, we decided to consider the mathematical model for the electrical propagation only on the endocardium (and not in the whole myocardum) given by the *isotropic* version of the Eikonal model, which reads

$$V_e \, |\nabla u_e| = 1 \quad \mathbf{x} \in \Omega_e, \qquad (1)$$
$$u_e(x) = u_{e,0}(x) \quad \mathbf{x} \in \Gamma_e,$$

where $u_e(\mathbf{x})$ is the unknown activation time at a point of the endocardium with coordinates $\mathbf{x}$, Ω_e is the computational domain, Γ_e is the set of points generating the front, that is the PMJ, $u_{e,0}(\mathbf{x})$ is the value of the activation times in Γ_e, and V_e is the velocity of the front, tuned in the range 0.3-0.8 m/s maximizing the agreement with the clinical measures. We observe that Ω_e is a surface, so that the gradient has to be intended as a the projection of the gradient onto the tangential plane at $\mathbf{x}$.
For the solution of equation (1) at step 4 of the algorithm, one needs to know the source term $u_{e,0}$ that represents the activation times at the PMJ. To obtain such values, the activation times in the PF tentative network must be known (step 3). Analogously, to compute the final electrical activity (step 8), one needs to know the activation times in the patient-specific network to provide the source terms to equation (1) (step 7). Therefore, we needed to introduce a mathematical model to compute the activation times also in a Purkinje network. With this aim, we considered again an isotropic Eikonal model, more precisely

$$V_p \, |\partial u_p / \partial s| = 1 \quad \mathbf{x} \in \Omega_p, \qquad (2)$$
$$u_p(x) = u_{p,0}(x) \quad \mathbf{x} \in \Gamma_p,$$

where $u_p(\mathbf{x})$ is the unknown activation time at the point of the network with coordinates $\mathbf{x}$, Ω_p is the computational domain representing the network, Γ_p is set of points generating the front (in the normal propagation the AV node), $u_{p,0}(\mathbf{x})$ represents the activation times in Γ_p, and V_p is the velocity of the front, supposed to be constant and tuned in the range 3-4 m/s, maximizing the agreement with the clinical measures. We observe that the computational domain Ω_p in this case is a line, so that the derivatives have to be intended as directed along the tangent *s*.
For the numerical solution of the Eikonal equations (1) and (2) we considered the Fast Marching Method [21], implemented in the software VMTK (www.vmtk.org).

Details of the patient-specific generation of the Purkinje fibers network
We provide here a few details of the algorithm described above.
At step 1, the bundle of His and the main bundle branches were manually designed, accordingly to anatomical *a priori* knowledge [1,18]. At step 2 a tentative network as a fractal tree was generated. The growing process followed the 'Y' production rule, similar to that implemented in [1,9,18], where the number of levels of the tree, the same for each branch, was determined *a priori*. In our approach, at each level of the generation, we identified *active branches* and *leaves*. An active branch can generate other branches, whereas leaves terminate at their end points which are identified with the PMJ. In this way, the branches could be characterized by a different number of levels. To ensure a correct distribution of the PMJ on the endocardium, we described the process of generation of a leaf by means of a Bernoullian probability, where the probability to generate a leaf, p, is a function of the tree level. In particular, p is small for the first levels and grows up for the successive levels. To obtain a more realistic pattern of PF, we described the lengths L_l and L_r and the branching angle α of the new fibers by means of Gaussian variables, with mean value 4.0±0.3 mm for the lengths and $60\pm1{,}8^0$ for the angle [18], see Figure 1.

Figure 1

Fig. 1 Schematic representation of the generation of two new branches in the Purkinje network. L_l, L_r and α indicate Gaussian variables

The active branches stopped to generate new branches when one or several of the following conditions were satisfied:

i) The active branches intersected other branches;

ii) The active branches reached the zone identified with the upper areas of the mid-antero septum (this region being not reached by the Purkinje network [19]);

iii) The maximum number of levels defined by the user has been reached.

This procedure allowed to generate a network which in what follows has been referred to as *tentative network*.
The activation times on the PMJ were then computed by solving the 1D Eikonal equation (2) in the tentative network (step 3). These activation times were then used as sources for the Eikonal problem (1) on the endocardium (step 4), allowing to obtain a tentative activation map which was then compared with the experimental data (step 5).
The algorithm passed then to the final stage, represented by step 6 and consisting in adapting the tentative network to the clinical data by using the discrepancies computed at step 5. Accordingly, the leaves of the network were moved or deleted in order to satisfy the data. This is a completely new step with respect to previous works in the generation of PF and allowed to obtain a patient-specific Purkinje network. In particular, for each point $\mathbf{x}_j$ where the measures were available, we defined its *region of influence* as the set S_j of PMJ which were possible sources determining the activation time t_j in $\mathbf{x}_j$ when solving a 2D Eikonal equation (1). In other words, PMJ not belonging to S_j did not contribute in determining the solution in $\mathbf{x}_j$. To do this, we proceeded as follows:

i) We solved a 2D *backward* Eikonal problem using the measures as sources;

ii) Given a PMJ p_i located in $\mathbf{y}_i$, we concluded that p_i belonged to S_j if it has been activated at step i) by the source located in $\mathbf{x}_j$.

This allowed to associate to any p_i an activation time τ, solution of the backward problem, which is nothing but the boundary condition which would guarantee that p_i activated the point $\mathbf{x}_j$ at time t_j (see Figure 2A). We then compared the activation time τ in PMJ p_i obtained by solving the backward problem with τ_i obtained by solving the network. If these two values were in agreement, we conclude that PMJ p_i is able to activate the measure located in $\mathbf{x}_j$. Otherwise, we moved p_i in order to minimize the mismatch between τ and τ_i (see Figure 2B). The code for the implementation of this algorithm has been written in C++ using the VTK 5.8 library.

Figure 2

Fig. 2 A) The first backward signal reaching PMJ p_i starts from measure $\mathbf{x}_j$ so that p_i belongs to the region of influence S_j; B) PMJ p_i is then moved in order to maximize the accordance between the activation time τ_i computed by the network and that predicted by the backward Eikonal solution τ

Models for a computational comparison

In order to assess the accuracy of the numerical solutions obtained with our strategy (referred in what follows to as model D), we compared its performance with that of other three scenarios used so far in the literature:

i) Absence of the Purkinje network and localization of a single source for problem (1) at the apex of the ventricle [16] (model A);

ii) Absence of the network and localization of the sources for problem (1) driven by the clinical measurements [20] (model B). In particular, we identified as source the points with the smallest measured activation times;

iii) Presence of the tentative network [1,9,18] (only steps 1,2,3,4 of our algorithm, model C).

RESULTS

In this section, we show the numerical results related to the normal propagation of the three subjects, referred in what follows to as subject 1, 2 and 3. The goal is to compare the measured activation times with those computed by the four scenarios considered for the comparison. Given a point on the endocardium where a measure was available, we say that the related datum has been *satisfied* by one of the four models if the difference in activation time between the datum and the computed value was less than 20%.

Our starting points were the geometries reconstructed from the MRI data and the measured activation times in the three subjects. We acquired such measures in 186 points for subject 1, in 156 points for subject 2 and in 284 points for subject 3.

Since we used a probabilistic model to generate the Purkinje tentative network, each run of our method produced a different outcome. For this reason, we ran the algorithm 20 times for subject, generating 20 tentative and 20 patient-specific networks. In Table 1, first two rows, we reported the mean number and the standard deviation of branches and PMJ in the generated networks. In Figures 3, for each of the subjects, at the top we indicated the localization of the sources for models A and B, whereas at the bottom we reported a selected network generated by our algorithm for each case. We observe that in all the three subjects by using model D no PMJ were generated at the base of the ventricle, as expected from the anatomical knowledge. Accordingly, the network generated in such a region was deleted. Therefore, for our method one does not need

to decide *a priori* which region of the base should be not reachable by the network (as needed when using model C) since the method itself is able to identify such a region.

Table 1

Figure 3

Fig. 3 Subjects 1, 2 and 3. Top. Localization of the sources in the models without PF: Model A (left) and model B (right). Bottom. Tentative (model C, left) and patient-specific (model D, right) Purkinje networks generated by our algorithm. In yellow we depicted the PMJ. For models C and D we depicted one selected case over the 20 simulated

Then, we solved the Eikonal problem (1) on the endocardium, obtaining the activation times for all the four models, reported in Figures 4, 5 and 6. For models C and D we depicted one selected case over the 20 simulated. The velocities of conduction in the network (V_p) and on the endocardium (V_e) have been tuned in order to maximize the number of satisfied points and it has been kept constant in the 20 simulations of models C and D. We reported such quantities in Table 1, third and fourth rows. We observe that for models C and D such values fell into the physiological ranges (3-4 m/s for V_p and 0.3-0.8 m/s for V_e). Regarding models A and B, the absence of the PF network has been supplied by choosing a conduction velocity V_e which could change over the domain. In particular, we chose two different values of such a velocity, one in the region of the endocardium which is activated by the PF, and another one in the region characterized by a purely muscular activation (that is at the base of the ventricle and at the upper areas of the mid-antero septum). From Table 1 we observe that for models A and B we let V_e assume values outside the muscular physiological range (but consistent with the conduction velocity in the network) to account for the PF propagation.
In Figures 4, 5 and 6 we also plotted the measured activation times (represented with squares) and the absolute error (that is the distance between computed and measured data) at each point. We observe an excellent qualitative agreement between measured and computed data obtained with our method, whereas a comparable accuracy was obtained by models B and D. Model A seemed to feature the poorest accuracy among the four models.
In order to quantify the accuracy of the different models, we computed the percentage of satisfied points and the average relative error in activation time between the measures and the prediction by the four models in each measurement point. We reported such values in Table 2, which confirmed the better accuracy of the model with a patient-specific Purkinje network (model D) with respect to the other models.

Table 2

Figure 4

Fig. 4 Computed activation times and errors for the four models. Top left, model A. Top right, model B. Bottom left, model C. Bottom right, model D. For each case, in the upper row we depicted the computed activation times (the measured data are plotted with squares), and in the lower row we represented the absolute errors. For models C and D we depicted one selected case over the 20 simulated. Subject 1, normal activation

Figure 5

Fig. 5 Computed activation times and errors for the four models. Top left, model A. Top right, model B. Bottom left, model C. Bottom right, model D. For each case, in the upper row we depicted the computed activation times (the measured data are plotted with squares), and in the lower row we represented the absolute errors. For models C and D we depicted one selected case over the 20 simulated. Subject 2, normal activation

Figure 6

Fig. 6. Computed activation times and errors for the four scenarios. Top left, model A. Top right, model B. Bottom left, model C. Bottom right, model D. For each case, in the upper row we depicted the computed activation times (the measured data are plotted with squares), while in the lower row we represented the absolute errors. For models C and D we depicted one selected case over the 20 simulated. Subject 3, normal activation

DISCUSSION

State of the art. Mathematical models of the cardiac electrophysiology allow to compute virtually the electrical activity in the ventricles, providing a non-invasive tool for the study of the propagation of the electrical signal [11]. Despite PF have an essential function in the coordinated activation of the ventricles, they have been usually neglected in the computational models [20]. This was mainly due to the difficulty in obtaining *in vivo* images of the PF, which are excessively thin for the current clinical imaging resolution.
A common strategy used so far to obtain significant results without generating explicitly the Purkinje network consisted in locating the source of the front at the apex of ventricle (model A) [16]. An alternative approach has been considered in [20], where the sources were localized by analyzing available clinical data and defining space-dependent conduction properties (model B).
Nevertheless, accounting for the PF in ventricular computational models is essential to simulate the normal activation [23,17]. For this reason, some scientists have attempted to incorporate PF in the mathematical models by their explicit construction. Three possible alternatives have been proposed so far:

(i) A manual procedure based on the anatomical knowledge [23,3] ;

(ii) The segmentation of PF from *ex vivo* images [4];

(iii) The construction of the Purkinje network computationally with a semi-automatic algorithm [1,9,18].

In the latter case, the network generation was driven only by general anatomical information and was not patient-specific (model C). In this work we proposed to use the same approach, where however *the construction of PF has been driven by clinical patient-specific data* concerning the activation times on the endocardium of a normal propagation (model D). At the best of our knowledge, this has been the first attempt to use clinical data for the explicit construction of the Purkinje network by means of computational tools, *allowing to obtain patient-specific networks*.

Discussion of the results. We applied the four models to three subjects characterized by a normal conduction activity (Figures 3,4,5,6 and Tables 1,2). Our results showed that the errors obtained with model B decreased in the three subjects by 14%, 10%, 74%, respectively, in comparisons of those obtained with model A, while the number of satisfied points increased by a factor 2.9, 13.0 and 1.5, respectively. This showed that the use of clinical data could improve the accuracy of the numerical results when no PF are modeled.
The same conclusion concerning the importance of using clinical data to improve the accuracy, holds also for the models with a Purkinje network. Indeed, the errors obtained with model D decreased in the three subjects by 41%, 55%, 49%, respectively, in comparisons of those obtained with model C, while the number of satisfied points increased by a factor 1.7, 2.5 and 1.5, respectively.
By comparing the performance obtained by models which exploited clinical measures (models B and D), we found that the inclusion of the Purkinje network is fundamental to obtain accurate results. Indeed, the errors obtained with model D decreased in the three subjects by 53%, 62%, 25%, respectively, in comparisons of those obtained with model B, while the number of satisfied points increased by a factor 2.0, 3.0 and 1.4, respectively.
Moreover, by comparing the accuracy of models B and C we found that such methods featured more or less the same accuracy. This showed that using the clinical data without modeling the Purkinje network or modeling the network without using the clinical data brought more or less to the same level of accuracy. *This clearly showed the importance of using both clinical data and a Purkinje network to obtain accurate results by numerical simulations of a normal propagation*.

On the choice of considering only the endocardium to generate the patient-specific network. In this work we considered the activation times related to a normal ventricle propagation. In such a

condition the electrical signal propagates firstly on the endocardium and then into the myocardium starting uniquely from the PMJ. Therefore, for a normal activation *the propagation in the myocardium does not influence that on the endocardium*. As observed, to generate the patient-specific Purkinje network we needed to know the activation times only on the endocardium (step 5 of our algorithm). These facts justified our choice to solve a problem only on the endocardium at step 4 of our algorithm.

On the choice of using the Eikonal model. Regarding the mathematical models used to compute the activation times (problems (1) and (2)), we considered in this work the Eikonal equation both for the PF and for the endocardium. In its more complex version, such equation accounts for the orientation of the muscular fibers and for the diffusion process characterizing the front (anisotropic Eikonal-Diffusion equation [14,20]). This model was proved to be a good approximation of the more complex bidomain one for computing the activation maps in the myocardium [6] and has been considered also for clinical applications [22].
In this work, we made two approximations for the Eikonal equation. From one hand, we considered the isotropic version of such a model. Indeed, as already noticed, for a normal activation the signal enters the ventricle at the level of the endocardium, propagating first on such a surface and then in the myocardium. Therefore, for a normal ventricle activation *the propagation on the endocardium is not influenced by the muscular fibers* which are located downstream, along the thickness of the myocardium, and not on the endocardium. This justified our choice of using the isotropic equation. On the other hand, we neglected the diffusion term, since we assumed that the diffusion process gives a small contribution with respect to the advection one. This was justified by noticing that PF were so dense to inhibit the diffusion to become relevant.
Concerning the propagation in the PF, these two approximations (isotropy and absence of diffusion) were perfectly justified, due to the absence of fibers (and then of anisotropy) in the network, and to the high advection term V_p which dominated any diffusion process.

On the versatility of the proposed method. The use of our method is independent of the model chosen to compute the electrical activity in the Purkinje network and in the endocardium at steps 3 and 4. Indeed, one could consider different models, for example the anisotropic Eikonal equation, the monodomain or the bidomain models. Then, steps 5 and 6 would follow as in the described case. This shows the versatility of our method which could be used in combination with different electrical models depending on the required accuracy and efficiency. In particular, in this work we showed that for a normal propagation the use of the isotropic Eikonal equation is enough to provide accurate results. However, in other situations, this could not be the optimal choice. For example, the premature muscular propagation characterizing the Wolff–Parkinson–White (WPW) syndrome is known to be caused by an anomalous conduction way (the bundle of Kent) which enters the left ventricle in an intramyocardial region. Therefore, in this case the signal reached the endocardium after having propagated through the myocardium through the muscular fibers. In such a case one should need to account for example for a 3D Eikonal model with anisotropy, since the muscular fibers would influence the propagation on the endocardium. This is currently under study and it will be the subject of future works.

CONCLUSIONS

In this work we proposed a method for the computation of a patient-specific Purkinje network starting from clinical measurements of a normal electrical propagation, to be used to improve the computational models for the computation of the electrical activity in the left ventricle. The main contributions of the present work are summarized in what follows:

- We showed, for the first time, the feasibility of using clinical measurements of the activation times on the endocardium to drive the Purkinje network generation by means of computational tools, allowing to recover patient-specific networks;

- We showed an improvement of the accuracy in the case of a normal propagation when patient-specific measures were used to drive the simulation, both in the absence and in the presence of a Purkinje network;

- We showed the importance of generating a patient-specific Purkinje network to recover an accurate electrical activation on the endocardium for a normal propagation, when clinical measures are available;

- We showed that the simple isotropic Eikonal model solved only on the endocardium was enough to describe accurately the normal propagation on such a surface.

These conclusions show us that the proposed method is able to provide an effective tool to improve the accuracy in the computation of the normal electrical activity of the left ventricle. The next step we are working on is the adaptation of such a method to the description of pathological cases such as WPW.

CONFLICT OF INTEREST

We state that there are no disclosures.

ACKNOWLEDGMENTS

The present study has been funded by Fondazione Cassa di Risparmio di Trento e Rovereto (CARITRO) within the project "Numerical modelling of the electrical activity of the heart for the study of the ventricular dissincrony".

REFERENCES

1. Abboud S, Berenfeld O, Sadeh D (1991) Simulation of high-resolution qrs complex using a ventricular model with a fractal conduction system. Effects of ischemia on high-frequency qrs potentials. Circ Res 68(6):1751-1760.
2. Anderson RH, Yanni J, Boyett MR, Chandler NJ, Dobrzynski H (2009) The anatomy of the cardiac conduction system. Clin Anat 22(1):99-113.
3. Berenfeld O, Jalife J (1998) Purkinje-muscle reentry as a mechanism of polymorphic ventricular arrhythmias in a 3-dimensional model of the ventricles. Circ Res 82(10):1063-1077.
4. Bordas R, Gillow K, Lou Q, Efimov IR, Gavaghan D, Kohl P, Grau V, Rodriguez B (2011) Rabbit-specific ventricular model of cardiac electrophysiological function including specialized conduction system. Prog Biophys Mol Biol 107(1):90-100.
5. Colli Franzone P, Guerri L (1993) Spreading excitation in 3-D models of the anisotropic cardiac tissue, I. Validation of the Eikonal Model. Math Biosci 113:145-209.
6. Colli Franzone P, Guerri L, Pennacchio M, Taccardi B (1998) Spread of excitation in 3-d models of the anisotropic cardiac tissue. II. Effects of fiber architecture and ventricular geometry. Math Biosci 147(2):131-171.
7. Colli Franzone P, Pavarino LF (2004) A parallel solver for reaction–diffusion systems in computational electrocardiology. Math Models Methods Appl 14(06):883-911.
8. Durrer D, van Dam RR, Freud GE, Janse MJ, Meijler FL, Arzbaecher RC (1970) Total excitation of the isolated human heart. Circulation 41(6):899-912.

9. Ijiri T, Ashihara T, Yamaguchi T, Takayama K, Igarashi T, Shimada T, Namba T, Haraguchi R, Nakazawa K (2008) A procedural method for modeling the Purkinje fibers of the heart. J Physiol Sci 58(7):481-486.
10. Keener JP (1991) An eikonal-curvature equation for action potential propagation in myocardium. J Math Biol 29(7):629-651.
11. Keener JP, Sneyd J (1998) Mathematical Physiology. New York, Springer.
12. Keener JP, Bogar K (1998) A numerical method for the solution of the bidomain equations in cardiac tissue. Chaos 8(1):234-241.
13. Kerckhoffs RC, Faris OP, Bovendeerd PH, Prinzen FW, Smits K, Arts T (2003) Timing of depolarization and contraction in the paced canine left ventricle: model and experiment. J Cardiovasc Electr 14(10 Suppl):S188-S195.
14. Pashaei A, Romero D, Sebastian R, Camara O, Frangi A (2011) Fast multiscale modeling of cardiac electrophysiology including purkinje system. IEEE T Biomed Eng 58(10):2956-2960.
15. Rawling DA, Joyner RW, Overholt ED (1985) Variations in the functional electrical coupling between the subendocardial purkinje and ventricular layers of the canine left ventricle. Circ Res 57(2):252-261.
16. Rodriguez B, Li L, Eason JC, Efimov IR, Trayanova NA (2005) Differences between left and right ventricular chamber geometry affect cardiac vulnerability to electric shocks. Circ Res 97(2):168-175.
17. Romero D, Sebastian R, Bijnens B, Zimmerman V, Boyle P, Vigmond E, Frangi A (2010) Effects of the Purkinje system and cardiac geometry on biventricular pacing: A model study. Ann Biomed Eng 38:1388-1398.
18. Sebastian R, Zimmerman V, Romero D, Frangi A (2011) Construction of a computational anatomical model of the peripheral cardiac conduction system. IEEE T Biomed Eng 58(12):3479-3482.
19. Sebastian R, Zimmerman V, Romero D, Sanchez-Quintana D, Frangi A (2012) Characterization and Modeling of the Peripheral Cardiac Conduction System. IEEE T Med Imaging. In press. DOI: 10.1109/TMI.2012.2221474.
20. Sermesant M, Chabiniok R, Chinchapatnam P, Mansi T, Billet F, Moireau P, Peyrat JM, Wong K, Relan J, Rhode K, Ginks M, Lambiase P, Delingette H, Sorine M, Rinaldi CA, Chapelle D, Razavi R, Ayache N (2012) Patient-specific electromechanical models of the heart for the prediction of pacing acute effects in CRT: a preliminary clinical validation. Med Image Anal 16(1):201-215.
21. Sethian JA (1999). Level Set Methods and Fast Marching Methods: Evolving Interfaces in Computational Geometry, Fluid Mechanics, Computer Vision, and Materials Science. Cambridge, Cambridge University Press.
22. Tobon-Gomez C, Duchateau N, Sebastian R, Marchesseau S, Camara O, Donal E, De Craene M, Pashaei A, Relan J, Steghofer M, Lamata P, Delingette H, Duckett S, Garreau M, Hernandez A, Rhode KS, Sermesant M, Ayache N, Leclercq C, Razavi R, Smith NP, Frangi AF (2013) Understanding the mechanisms amenable to CRT response: from pre-operative multimodal image data to patient-specific computational models. Med Biol Eng Comput. doi 10.1007/s11517-013-1044-7.
23. Tusscher KH, Panfilov AV (2008) Modelling of the ventricular conduction system. Prog Biophys Mol Biol 96(1-3):152-170.
24. Vigmond EJ, Aguel F, Trayanova NA (2002) Computational techniques for solving the bidomain equations in three dimensions. IEEE Trans Biomed Eng 49(11):1260-1269.

		model A	model B	model C	model D
SUBJECT 1	**# branches**	X	X	1977±42	1724±46
	# PMJ	X	X	494±13	239±10
	V_p (m/s)	X	X	3.9	3.9
	V_e (m/s)	2.4/0.8	2.4/0.8	0.6	0.6
SUBJECT 2	**# branches**	X	X	1382±30	1218±51
	# PMJ	X	X	343±12	179±39
	V_p (m/s)	X	X	3.9	3.9
	V_e (m/s)	2.4/0.8	2.4/0.8	0.6	0.6
SUBJECT 3	**# branches**	X	X	2521±102	2149±100
	# PMJ	X	X	611±34	240±26
	V_p (m/s)	X	X	3.2	3.2
	V_e (m/s)	2.3/0.8	1.6/0.8	0.4	0.4

Table 1. Number of branches and of PMJ of the networks generated by models C and D, and estimated conduction velocities in the network (V_p) and on the endocardium (V_e). For V_e in models A and B the first value refers to the endocardium excluding the base of the ventricle and the upper areas of the septum, while the second one refers to the base of the ventricle and the upper areas of the mid-antero septum. For models C and D the results have to be intended as the average over the 20 simulations

		SATISFIED POINTS (%)	MEAN RELATIVE ERROR (%)
SUBJECT 1	**model A**	11.2	50.0±5.5
	model B	32.8	43.0±6.3
	model C	39.9±2.3	33.9±6.8
	model D	66.7±1.5	19.9±5.3
SUBJECT 2	**model A**	1.6	83.8±12.4
	model B	20.8	75.5±9.0
	model C	25.3±3.9	63.9±8.6
	model D	63.1±2.4	28.6±6.0
SUBJECT 3	**model A**	31.7	103.4±12.3
	model B	47.1	26.7±4.9
	model C	43.3±4.5	39.1±5.5
	model D	64.1±4.1	20.1±4.6

Table 2. Percentage of satisfied points (that is characterized by an error less than 20%) and mean relative error for the three cases in the four scenarios. For models C and D the results have to be intended as the average over the 20 simulations

FIGURE 1

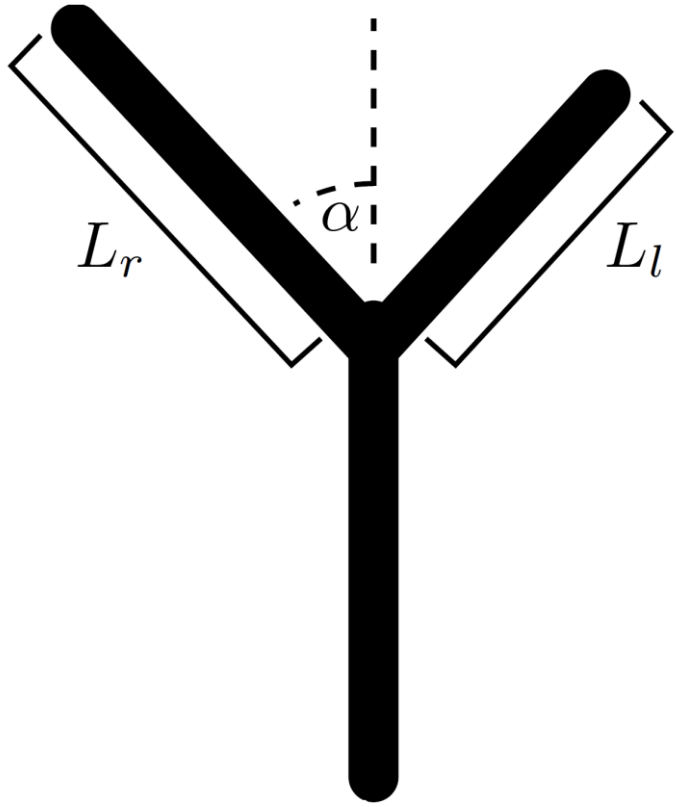

FIGURE 2

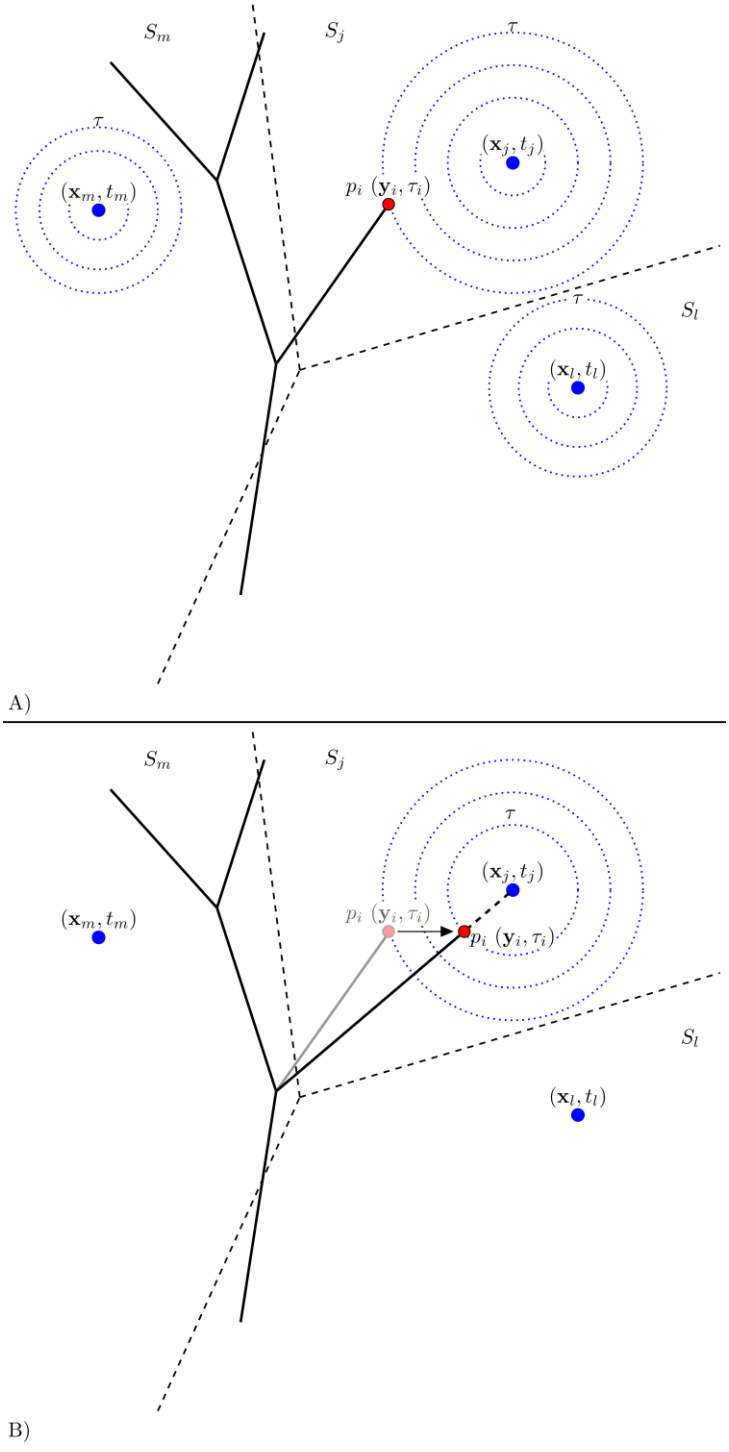
S_m
S_j
τ
τ
$(\mathbf{x}_j, t_j)$
$(\mathbf{x}_m, t_m)$
p_i $(\mathbf{y}_i, \tau_i)$
τ
S_l
$(\mathbf{x}_l, t_l)$
A)
S_m
S_j
τ
$(\mathbf{x}_j, t_j)$
$(\mathbf{x}_m, t_m)$
p_i $(\mathbf{y}_i, \tau_i)$
p_i $(\mathbf{y}_i, \tau_i)$
S_l
$(\mathbf{x}_l, t_l)$
B)

FIGURE 3

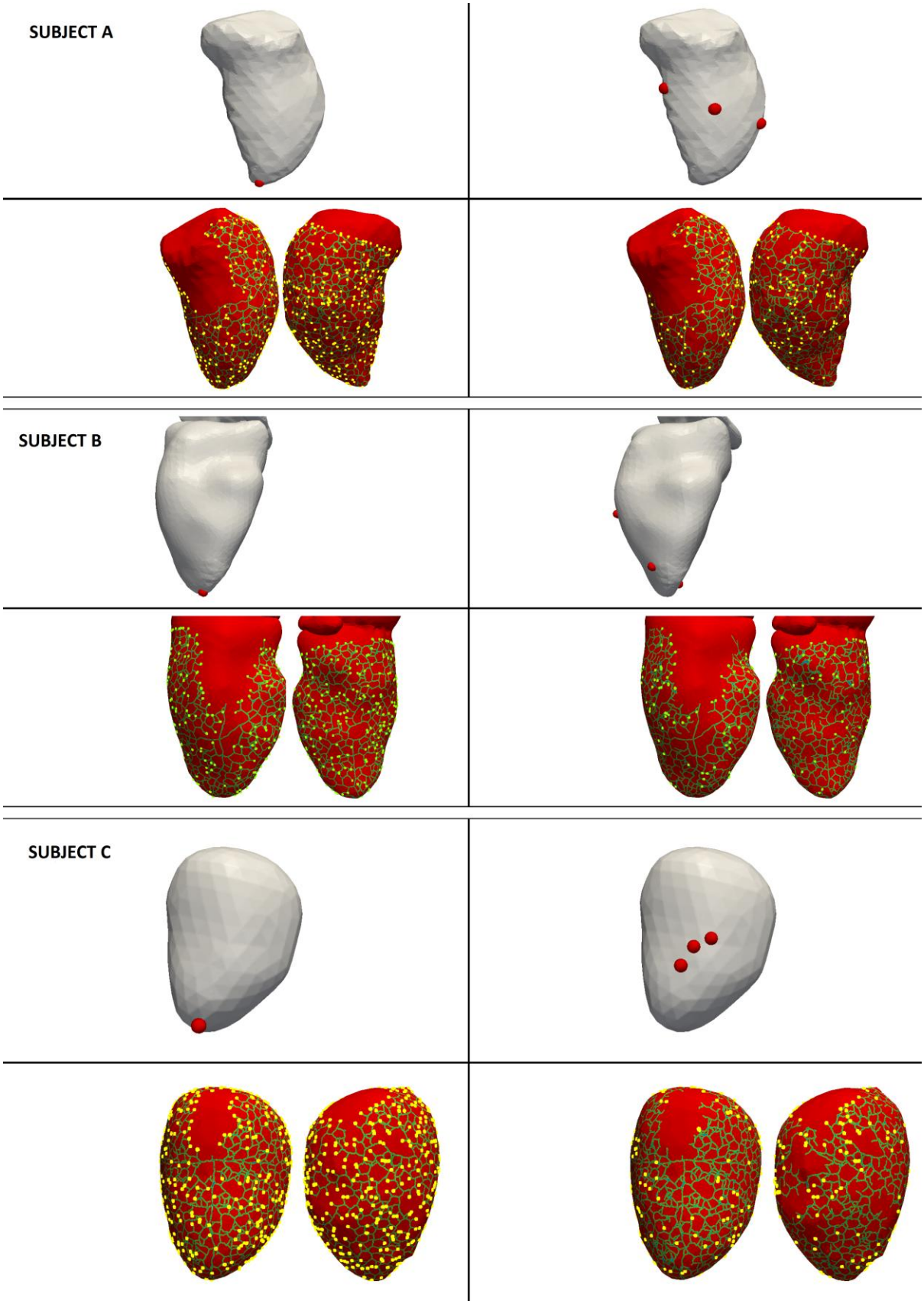

FIGURE 4

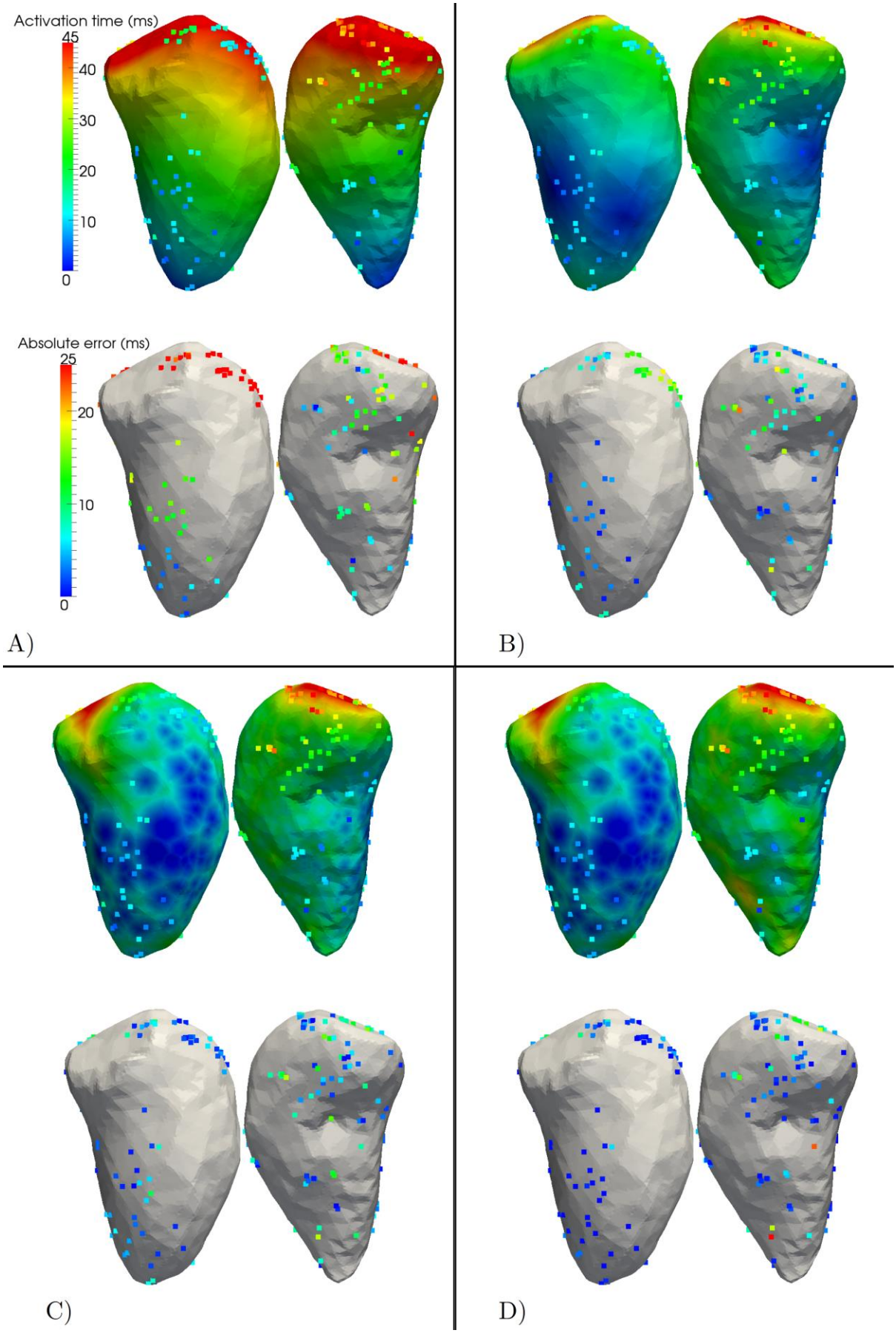
Activation time (ms)
45
40
30
20
10
0
Absolute error (ms)
25
20
10
0
A)
B)
C)
D)

FIGURE 5

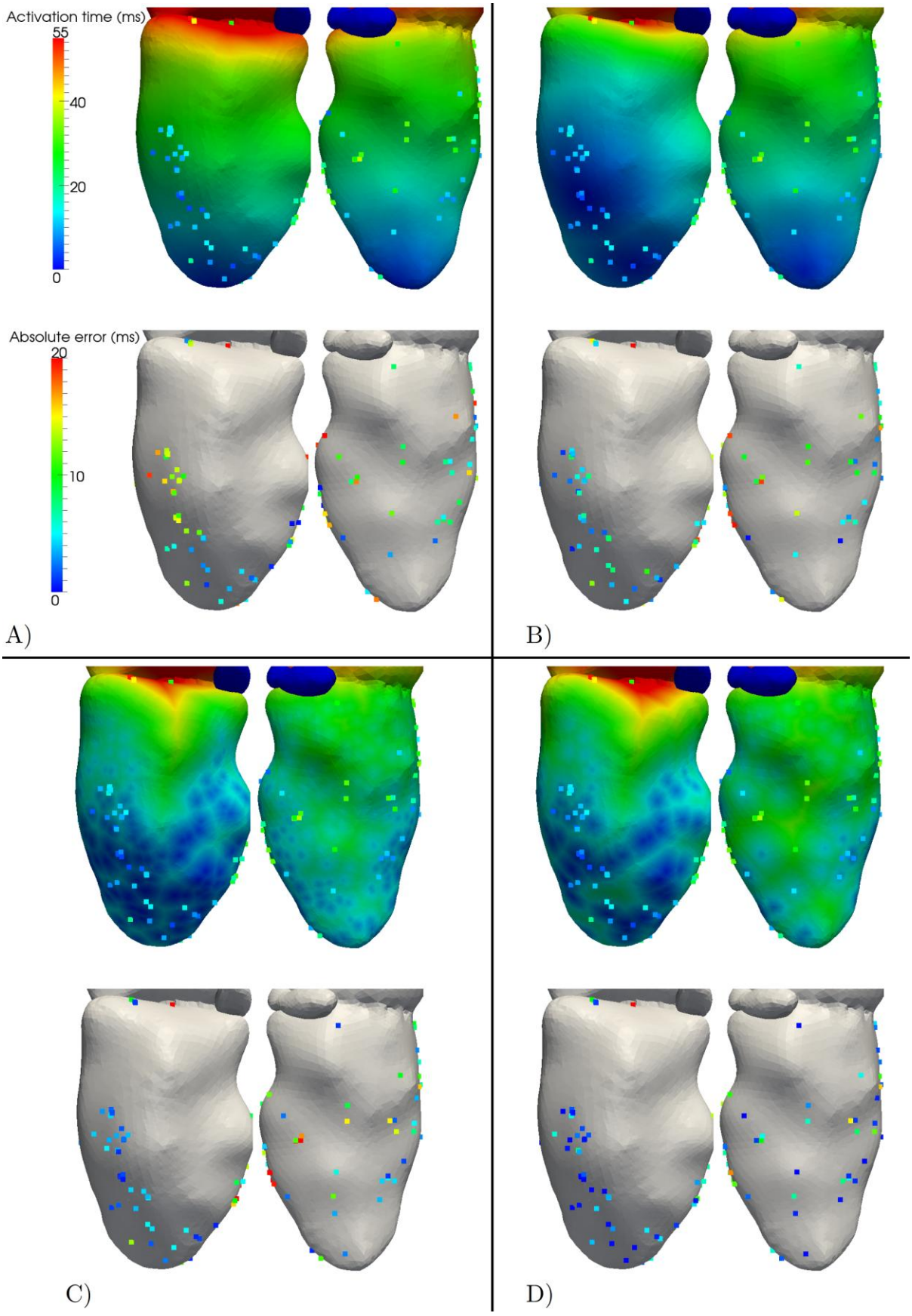

FIGURE 6

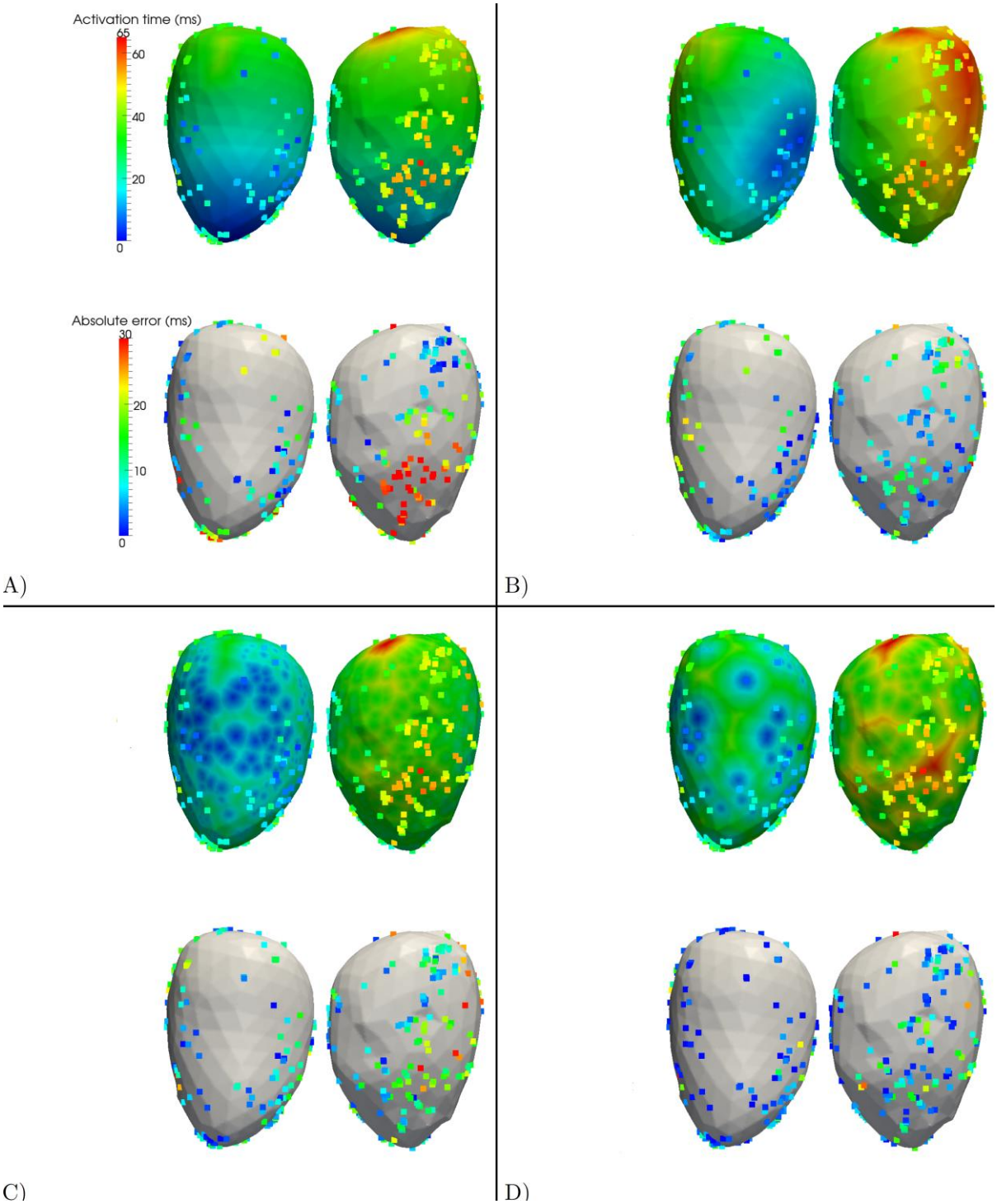
Activation time (ms)
65
60
40
20
0
Absolute error (ms)
30
20
10
0
A)
B)
C)
D)